

**CARBONATION-INDUCED CORROSION OF BLENDED-CEMENT
CONCRETE MIX DESIGNS FOR HIGHWAY STRUCTURES**

Eric I. Moreno* and Alberto A. Sagués
Department of Civil and Environmental Engineering
University of South Florida
4202 E. Fowler Avenue
Tampa, Florida 33620

*Permanent Affiliation: CINVESTAV-Mérida Unit, México

ABSTRACT

Corrosion of concrete reinforcing steel in highway structures has traditionally been related to chloride ions. However, another cause of reinforcing steel corrosion is concrete carbonation which decreases the pH of the pore solution. Carbonation-induced corrosion tends to develop later and proceeds at slower rates than chloride-induced corrosion. Since very long service life goals are currently proposed for new highway structures, concrete carbonation is a likely concern when projecting durability. The objective of this investigation was to establish the prognosis for development of carbonation-induced corrosion of concrete mix designs proposed for new construction projects. Accelerated laboratory carbonation exposures to 60% relative humidity with 0.5% and 4% CO₂ were conducted with concrete mix designs containing from 20% to 50% pozzolanic cement replacement, 2 different water-to-cementitious ratios, and with small levels (~2 kg/m³) of Cl⁻ contamination (non-contaminated specimens were also included). Both the carbonation and the electrochemical behavior were monitored as a function of time. Carbonation rates were found to be directly dependent on the pozzolanic content. Polarization Resistance measurements showed that steel corrosion rates at 60% RH were small where chloride contamination was not present but increased to ~0.2 μA/cm² with moderate Cl⁻ contamination. Corrosion rates increased by over one order of magnitude for all mixes (except a low water-to-cementitious ratio, 20% pozzolanic cement replacement mix) during a post-carbonation high humidity exposure.

Keywords: carbonation, concrete, corrosion, fly ash, rebar, silica fume

INTRODUCTION

Corrosion of steel in concrete is usually related to chloride ions from seawater or deicing salts. This problem has encouraged extensive research to improve design and concrete quality to retard chloride intrusion. Service lives approaching a 75-year design goal appear now to be achievable. However, the

Copyright

improvement in controlling chloride-induced damage has led to concern about another rather slow cause of steel depassivation: carbonation of concrete. Concrete carbonation results from the reaction of the hydrated cement compounds with atmospheric carbon dioxide which is present at a concentration of ~ 0.03%. Due to this reaction, the usually high pH (>12) of the concrete pore solution decreases to a level where the passivity of the steel is no longer sustained and general corrosion develops.¹ On first approximation concrete carbonation penetrates inward to a depth x proportional to the square root of the exposure time t ,

$$x = k \cdot t^{1/2} \quad (1)$$

where k is called the carbonation coefficient.²

In recent years, pozzolanic-blended cement have been used to improve chloride-corrosion resistance of concrete mixes. The pozzolanic addition slows down the Cl^- ingress due to a reduction in concrete permeability³ which follows the reaction of the pozzolanic material with the calcium hydroxide from cement hydration. However, concrete carbonation is fast if the amount of calcium in the concrete matrix is low.⁴ Therefore, blended-cement concrete mixes with low-calcium pozzolanic material could carbonate faster than plain-cement concrete mixes. This could be a disadvantage of candidate concrete mixes for present and future highway construction, which often contain pozzolanic admixtures.⁵ The aim of this investigation is to establish the prognosis for carbonation-induced corrosion in present and experimental concrete mixes for future long term durability applications.

EXPERIMENTAL PROCEDURE

Specimens and Materials

The cementitious materials used involved type I cement, class "F" fly ash, and silica fume. All materials satisfied AASHTO specification for the Florida Department of Transportation (FDOT) construction. The mix designs used are shown in Table 1. Mix designs A, D, and E have a total cementitious content (444 kg/m^3) representative of current FDOT concrete mixtures for marine substructure applications. Both plain and reinforced concrete specimens were used.

TABLE 1
CONCRETE MIX DESIGN

Mix	Cementitious Material	Mix Name	Water-to-Cementitious Ratio	Admixture to Cement Ratio
A	80% PC + 20% FA	Base	0.37	0.25
B	80% PC + 20% FA	High W/C	0.50	0.25
C	80% PC + 20% FA (0.4% Cl^-)*	Cl^-	0.50	0.25
D	72% PC + 20% FA + 8% SF	SF	0.37	0.39
E	50% PC + 50% FA	High FA	0.37	1.00

PC: Portland Cement; FA: Fly Ash; SF: Silica Fume.

* Cl^- % by weight of cementitious content.

The reinforced concrete specimens were rectangular prisms (50 mm deep, 100 mm wide, and 200 mm high), with 2 parallel rebars of the same type, protruding out of the top end. The rebar surface near the exit points was masked with a thick epoxy layer. The rebar specimens were size No. 3 (nominal 9.5 mm

diameter), 203 mm long with a 102 mm unmasked length (surface area 30.3 cm²) directly in contact with concrete. The rebars were cast 50 mm apart in the concrete specimens. An activated Ti rod reference electrode⁶ (3 mm diameter, 38 mm long), was cast in the center of each concrete specimen.

Plain concrete specimens were cylindrical in shape (75 mm diameter and 150 mm high). Six reinforced and 14 plain concrete specimens were cast per mix design and cured for 14 days in their molds. After curing, half of the specimens were allowed to dry in the lab environment (about 60% RH, 22°C) for about 100 days and then exposed to a 0.5% CO₂ environment for over 1100 days. The other half were allowed to dry in the same lab environment for about 750 days before exposing them to a 4% CO₂ environment.

The reinforced specimens were removed from the 4% CO₂ environment chamber after 200 days. They were placed again in the lab environment for about 120 days and then placed in a moisturizing chamber (90%±5% RH) to investigate corrosion rates at high humidity.

Carbonation Chamber

A carbonation chamber was built to hold 15 reinforced and 15 plain concrete specimens. To obtain the desired CO₂ concentration and RH inside the chamber, a flowing mix of pure carbon dioxide and air at two different moisture levels was used. The flow rates of the dry and wet air were adjusted periodically to maintain a 60%±5% RH inside the chamber. The CO₂ flow rate was adjusted accordingly.

Half Cell Potentials

Half cell potentials were taken regularly for each rebar against the internal reference electrode. This internal reference electrode was calibrated before starting the exposure period against an external copper-copper sulfate electrode (CSE) placed momentarily against the external concrete surface.

Polarization Resistance

Conventional polarization resistance tests were performed only on the rebar specimens that were kept in the 4% CO₂ environment (high concrete resistance values precluded reliable measurements in the specimens kept in the 0.5% CO₂ environment). The tests were conducted by varying the potential (starting from the open circuit value) in the negative direction, at a scan rate of 0.01 mV s⁻¹, to minimize possible capacitive effects.⁷ One rebar (identified as X-bar) was used as working electrode (WE); the other rebar (Y-bar) was always used as the counter electrode (CE); the activated Ti electrode was used as a reference electrode (RE) during the test. The test was interrupted when the potential became 10 mV more negative than the starting potential. The apparent polarization resistance was obtained from the slope of the potential-current curve at the maximum potential deviation. Surface-normalized apparent polarization resistance values were obtained by multiplying the apparent polarization resistance by the nominal specimen exposed metal area (30.3 cm²). All conversions to nominal corrosion current densities and corrosion rates were made after compensation for IR drop effects. A Stearn-Geary constant B = 26 mV was used to convert polarization resistance values into current densities.⁸

Carbonation depth measurements

Two plain concrete specimens per mix design were retrieved from the chamber at different times (at 121, 257, and 545 days for the specimens in the 0.5% CO₂ chamber, and at 29, 50, and 84 days for the specimens in the 4% CO₂ chamber). An ~50 mm slice was split from each concrete cylinder and a 1%

phenolphthalein solution was mist-sprayed over the newly broken concrete surfaces. Carbonation depth measurements were taken at different points from the circumference. The cylindrical-geometry carbonation depth measurements were converted to equivalent plane geometry values, using the procedure in Ref. 9. The remaining portion of the concrete cylinders were placed back in the chamber after the measurements.

RESULTS

Figure 1 shows the average potential behavior of the rebar specimens kept in the 0.5% CO₂ chamber. Each data point is the average of six different rebar specimens. The negative times correspond to the conditioning period before the CO₂ exposure. The Cl⁻ mix was the only concrete mix where the rebars showed a transition (which started on day ~200) of more than 200 mV toward less positive values. The rebars from mixes *High W/C* and *High FA* showed less pronounced potential changes also starting on day ~200. Minor potential fluctuations were observed for mix *SF* after day ~500. The potential in the *Base* mix remained virtually unchanged.

Figure 2 shows the potential evolution with time of the rebar specimens (average of six) in the 4% CO₂ chamber. Four time periods should be noted: the conditioning period ($t < 0$); the CO₂ exposure period up to day 200; the intermediate lab exposure (days 200 - 320); and the final period where the specimens were exposed to high RH. Starting on day ~25 of the CO₂ exposure period the potential of the rebar in both the Cl⁻ and *High FA* concrete mixes became significantly more negative. Less pronounced potential transitions started shortly afterwards for mixes *High W/C* and *SF*. The potentials tended to stabilize or recover during the intermediate period, and became more negative again upon exposure to high humidity (with the exception of the *Base* mix, which showed little change throughout).

Average apparent corrosion current densities are shown in Figure 3 for the specimens in the 4% CO₂ chamber. During the accelerated test only the rebars from the Cl⁻ mix showed current densities above 0.2 μA/cm², a value which has been proposed as indicative of active corrosion of steel embedded in atmospherically exposed concrete.¹⁰ The rebars from the remaining mixes had current densities in the range ~0.001 to ~0.01 μA/cm². In all 5 mixes the current densities tended to decrease with time. When the specimens were placed in the 90%±5% RH chamber all the current densities increased at least one order of magnitude (except in the *Base* mix). The current density reached 1 μA/cm² for the rebars in the Cl⁻ mix and ~0.2 μA/cm² for those in the *High FA* mix. The current densities were ≤ 0.06 μA/cm² in the other concrete mixes.

TABLE 2.
CARBONATION COEFFICIENTS (mm/y^{1/2})

Concrete Mix	k _{0.5} [0.5% CO ₂ Exposure]				k _{4.0} [4% CO ₂ Exposure]			
	121 days	257 days	545 days	Avg.	29 days	50 days	84 days	Avg.
Base	13.9	13.4	12.0	13.1	39.4	41.1	33.2	37.9
High W/C	19.6	18.7	18.8	19.0	54.1	51.8	50.6	52.1
Cl ⁻	20.1	20.1	19.8	20.0	52.9	49.3	46.3	49.5
SF	18.1	16.6	15.8	16.8	41.9	38.4	36.1	38.8
High FA	21.7	22.0	18.1	20.6	51.6	46.8	42.8	47.1

Table 2 shows the carbonation coefficients obtained from the carbonation depth measurements for each exposure condition at three exposure times. Each value corresponds to an average carbonation depth from 2 specimens. The carbonation coefficients decreased moderately with exposure time. For comparison purposes, the average of the measurements at the three exposure times will be used.

DISCUSSION

Carbonation Coefficients

Simplified modeling of the carbonation process^{9,11} shows that on first approximation the carbonation coefficient k is proportional to the square root of the CO_2 concentration in the external gas phase. Thus the average carbonation coefficients $k_{0.5}$ and $k_{4.0}$ in Table 2 may be converted to a nominal atmospheric carbonation coefficient k_a (for a concentration of 0.03%) by multiplying by $(0.03/0.5)^{1/2}$ and $(0.03/4.0)^{1/2}$ respectively. The conversions (Table 3) show reasonably good agreement between the results of both experiments and support the approximate validity of the square root concentration dependence.

TABLE 3
NOMINAL ATMOSPHERIC (0.03%) CARBONATION COEFFICIENTS k_a (mm/y^{1/2})

Concrete Mix	From 0.5% CO_2 Exposure	From 4% CO_2 Exposure
Base	3.21	3.28
High W/C	4.66	4.51
Cl ⁻	4.90	4.29
SF	4.12	3.36
High FA	5.05	4.07

Potential-Time Evolution

The time for carbonation penetration to a given depth is expected (from Eq.(1)) to be inversely proportional to k^2 . Based on the square root concentration dependence of k established above, the exposure time at 0.5% CO_2 needed to observe a given effect at the rebar depth should be approximately 8 times longer than at 4.0% CO_2 . This was tested by plotting the potential data in the CO_2 exposure period of Figure 2 against the variable $t' = 8 t_{4.0}$, where $t_{4.0}$ is the actual time of exposure at 4% CO_2 . The result (Figure 4) roughly approaches the trends and time scale for 0.5% CO_2 shown in Figure 1, and lends further credence to the approximate validity of the assumptions made.

Resistance to Carbonation Penetration

The potential transitions are an indication of the combined effects of local pH change and the onset of steel activity, following reduction of pH as concrete neutralization reaches the rebar depth.¹² The onset of a potential transition may therefore serve as an indicator of carbonation of the rebar surroundings. Likewise, the length of time required for the start of the transition could serve as a qualitative indication of the carbonation resistance of the concrete. The carbonation coefficient trends in Table 1, and the potential-time behavior in Figures 1 and 4 gave consistent indications of the relative resistance to carbonation of the concretes examined.

The two mixes with the highest water-to-cementitious ratio (*High W/C* and *Cl⁻*) were among those with the largest carbonation coefficients and showed the earliest rebar potential transitions. This was as expected since a high w/c ratio is normally associated with high porosity and permeability, and consequently faster carbonation. The moderate *Cl⁻* addition did not seem to have had any significant effect on the carbonation penetration.

Even though it had a low w/c ratio, the *High FA* mix also exhibited a large carbonation coefficient and early rebar potential transition. Two factors are expected to have facilitated rapid progression of the carbonation front in the *High FA* mix. Firstly, the CaO content (and corresponding Ca(OH)₂ content) was less than in the other mixes. Secondly, relative to the other mixes, the already low Ca(OH)₂ content was further reduced after hydration by the demand of a larger ash replacement.

The *Base* mix, which had a low w/c ratio and moderate pozzolanic replacement, had the lowest carbonation coefficient and the latest (if any) potential transition. The *SF* mix had an equally low w/c ratio and 8% SF, normally expected to result in highly dense concrete with superior resistance to the penetration of aggressive species.¹³ However, the *SF* mix had a carbonation coefficient and potential transition trends intermediate between that of the *Base* mix and the less resistant mixes. This behavior may be the result of the same factors mentioned for the *High FA* mix, with a lesser effect because of the intermediate level of cement replacement.

Corrosion Behavior

The polarization resistance results (Figure 3) suggest that the only significant corrosion during the carbonation exposure was taking place in the chloride-contaminated concrete, and at a quite low apparent rate. This low rate is likely to have resulted from reduced electrolyte availability since RH was only 60%. This interpretation is supported by the sharp increase in the apparent corrosion rate upon placement in the high humidity chamber. At the high humidity also the steel in the *High FA* mix exhibited some modest but significant indication of corrosion. Visual inspection of a selected *High FA* mix specimen showed complete carbonation of the concrete along with corrosion products on ~10% of the steel surface area. The presence of chloride ions may induce a higher corrosion rate in the *Cl⁻* mix than the *High FA* mix, by promoting various conditions. These include a larger fraction of the steel surface in the active condition, higher conductivity of the pore water, and an increase in the hygroscopic tendency of the concrete that would cause more electrolyte to be present. During the high humidity period the steel in the *High W/C* and *SF* mixes had apparent corrosion rates only marginally significant. Inspection of a selected *Base* mix specimen revealed an uncarbonated region between the two rebars and only a small corrosion area at the bottom end of one of the rebars. The lack of complete carbonation around the rebars may explain in part the low apparent steel corrosion rate observed in this mix.

Relative Overall Performance

The *Base* mix had the lowest carbonation coefficient. This is encouraging as the *Base* mix represents the class of concretes currently specified for construction in chloride environments classified as highly aggressive by the FDOT. In absolute terms, the *Base* mix value of $k_a \sim 3.3 \text{ mm/y}^{1/2}$ promises good performance (75 years to penetrate ~29 mm cover). In addition, this type of estimate is conservative as the values of k_a in Table 3 correspond to the worst condition of continuous exposure to 60% RH, for which carbonation is expected to progress fastest.¹¹ The *SF* mix (of a class also specified by FDOT for certain aggressive environments) showed slightly lesser performance than the *Base* mix but still promising when considering both the initiation and propagation stages of corrosion. Increasing the

pozzolanic replacement level to 50% appreciably increased the rate of carbonation penetration and also the rate of corrosion during the high humidity regime. This effect was worse than that of increasing the w/c ratio to 0.5 while limiting the pozzolanic replacement to 20%. The carbonation effect on corrosion in the chloride-contaminated concrete underscored the importance of avoiding the simultaneous action of both aggressive agents.

CONCLUSIONS

1. Concrete mixes with moderate pozzolanic replacement (< 28%) and low w/c (0.37) had the lowest carbonation coefficients. When humidity was increased after carbonation, steel in these mixes experienced very low corrosion rates (although in the *Base* mix this may be due in part to incomplete carbonation).
2. Carbonation coefficients were high for moderate cement replacement (20%) and high w/c, or for high cement replacement (50%) and low w/c. Chloride addition (2 kg/m³) did not affect the carbonation coefficient.
3. When humidity was increased, the highest corrosion rates were for the chloride containing mix and for the 50% cement replacement mix.

ACKNOWLEDGMENTS

This investigation was supported by the Florida Department of Transportation. The opinions, findings, and conclusions expressed here are those of the authors and not necessarily those of the Florida Department of Transportation. One of the authors (E.I.M.) acknowledges the scholarship provided by the National Council for Science and Technology (CONACyT-México).

REFERENCES

1. R. Bakker, in *Corrosion of Steel in Concrete*, ed. P. Schiessl (London, UK: Chapman and Hall, 1988), p. 22.
2. H. Weber, *Betonwerk+Fertig.*, 49, 8 (1983): p. 508.
3. R. Malek, D. Roy, and Y. Fang, in *Pore Structure and Permeability of Cementitious Materials*, eds., L. Roberts and J. Skalny (Pittsburgh, PA: Materials Research Society, 1989), p. 403.
4. K. Tuutti, *Corrosion of Steel in Concrete* (Stockholm, Swed: Swedish Cement and Concrete Research Institute, 1982).
5. P. Bamforth, *Concrete*, 28, 6 (1994): p. 18.
6. P. Castro, A. Sagüés, E. Moreno, L. Maldonado, J. Genésca, *Corrosion*, 52, 8 (1996): p. 609.
7. A. Sagüés, S. Kranc, and E. Moreno, *Corros. Sc.*, 37, 7 (1995): p. 1097.
8. C. Alonso and C. Andrade, *Adv. Cem. Res.*, 1, 3 (1988): p. 155.

9. E. Moreno, "Accelerated Carbonation-Induced Corrosion of Reinforcing Steel Bars in Blended-Cement Concrete," Master's Thesis, University of South Florida, May 1996.
10. C. Andrade and M. Alonso, in Application of Accelerated Corrosion Tests to Service Life Prediction of Materials ASTM STP 1194, eds., G. Cragolino and N. Sridhar (Philadelphia, PA: American Society for Testing and Materials, 1994), p. 282.
11. V. Papadakis, C. Vayenas, and M. Fardis, ACI Mats. J., 88, 4 (1991): p. 363.
12. C. Alonso and C. Andrade, Mats. Constr. (Madrid), 37, 206 (1987): p. 5.
13. N. Berke and M. Hicks, in Corrosion Forms and Control for Infrastructure ASTM STP 1137, ed., V. Chaker (Philadelphia, PA: American Society for Testing and Materials, 1992), p. 207.
14. A. Sagüés, H. Perez-Duran, and R. Powers, Corrosion, 47, 11 (1991): p. 884.

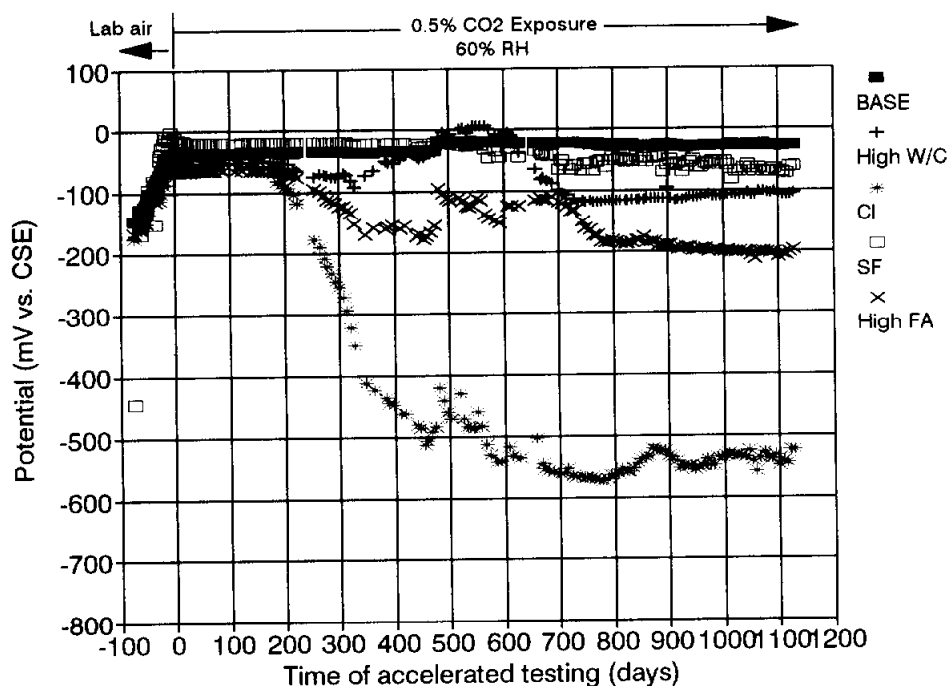


Figure 1. Potentials as a function of exposure time in the 0.5% CO₂ environment.

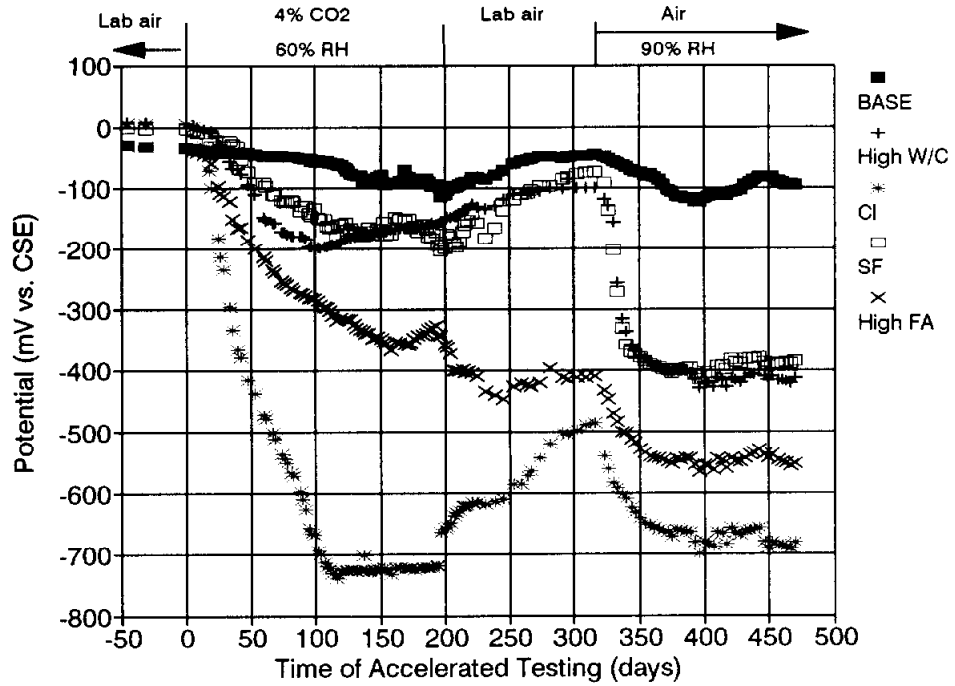


Figure 2. Potentials as a function of exposure time in the 4% CO₂ environment.

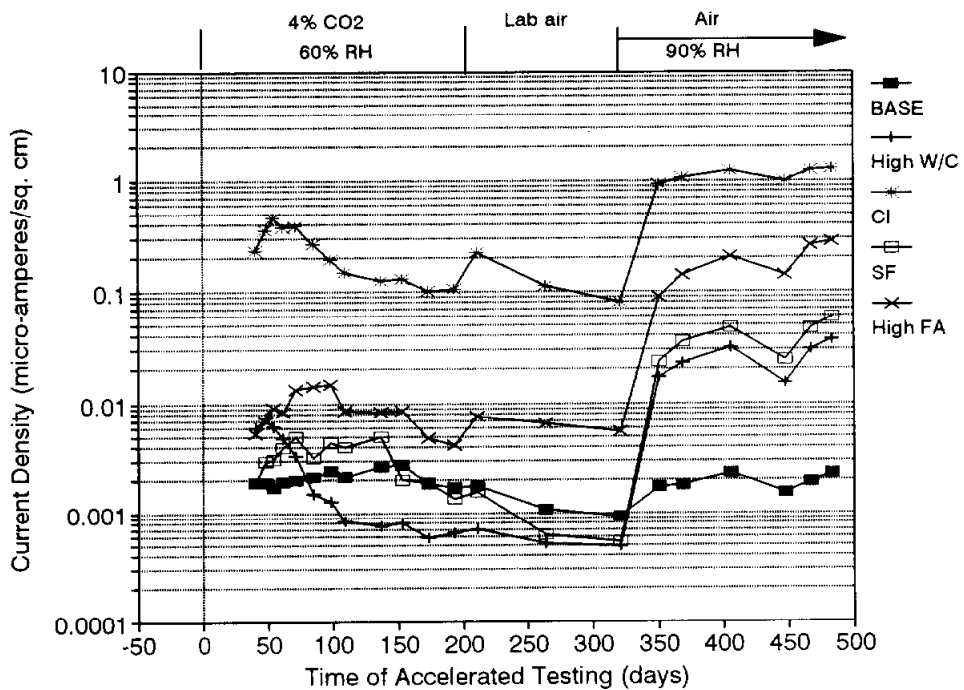


Figure 3. Average apparent current densities as a function of exposure time in the 4% CO₂ environment.

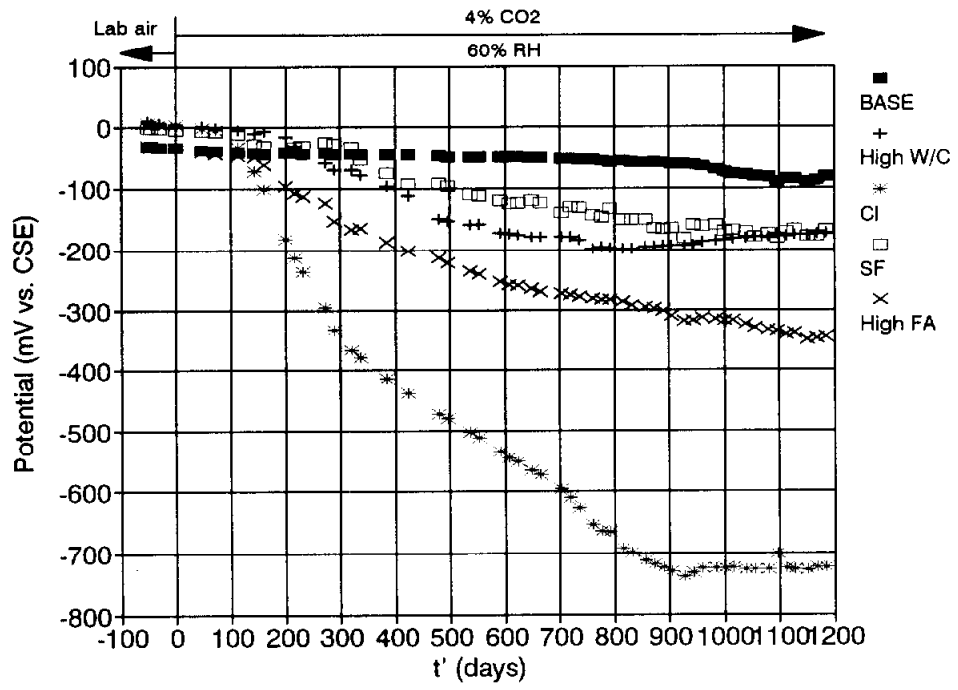


Figure 4. Potential evolution as a function of variable t' in 4% CO₂ environment ($t' = 8 t_{4.0}$).